Lithogenic mixing model approach identifies saprolite as the source of inorganic colloids in a granitoid catchment

By:

Noah Laeh Hoffman

B.A., Oberlin College, 2015

A thesis submitted to the

Faculty of the Graduate School of the

University of Colorado in partial fulfillment

of the requirement for the degree of

Master of Arts

Department of Geography

2019

This thesis entitled: Lithogenic mixing model approach identifies saprolite as the source of inorganic colloids in a granitoid catchment

written by Noah Laeh Hoffman

has been approved for the Department of Geography

_____

Suzanne Anderson

_____

Boswell Wing

_____

Holly Barnard

_____

Date

The final copy of this thesis has been examined by the signatories, and we find that both the content and the form meet acceptable presentation standards of scholarly work in the above mentioned discipline.

Abstract

Hoffman, Noah Laeh (M.A., Geography)
Lithogenic mixing model approach identifies saprolite as the source of inorganic colloids in a granitoid catchment
Thesis directed by Dr. Suzanne Anderson

The production and export of inorganic colloids in environmental systems affects soil formation, biogeochemistry, and geomorphology. Inorganic colloids also carry otherwise immobile contaminants through the critical zone. While theoretical and experimental work has described how colloids move through porous media, no framework has been developed to predict inorganic colloid sources based on critical zone properties, such as soil type. I develop a method of rapidly investigating colloid sources in a granitoid headwater catchment and employ it to predict where colloids are produced in its weathering profile. I develop a two-component mixing model of stream water chemistry using end-members based on the mineral stability of two groundwater wells, one screened partially in saprolite and one screened entirely in bedrock. I find that colloids are more abundant in stream water when saprolite water dominates, during spring meltwater flow. The relationship between colloid abundance and saprolite water is strongly non-linear at the outlet of the catchment. I describe a conceptual model of inorganic colloid production and export in the catchment based on my findings and prior work in the catchment. I predict that colloids are produced in the mobile regolith and upper saprolite, and stored in and exported to stream water from the mid to upper saprolite.

Acknowledgements

Thank you to my advisor, Suzanne Anderson, my committee, Boz Wing and Holly Barnard, and professors Eve Lyn-Hinckley and Alexis Templeton for your support and advice—I deeply appreciate your time and help.

Thank you to my mom for being my woman scientist role model and both my parents for their continual support.

Thank you to my friends and communities at CU, in Boulder, and across the U.S., you know who you are, let's explore again soon. Special shout out to friends and colleagues Anna Hermes, Stephanie Jarvis, Kate Travis, Lauren Lynch, and Ruth Heindel.

Thank you to the staff of the Boulder Creek Critical Zone Observatory for collecting this data and for being incredibly helpful.

Institutional support: Department of Geography at the University of Colorado Boulder, Institute of Arctic and Alpine Research, Boulder Creek Critical Zone Observatory

Contents

Introduction……1

Field site……5

Field site hydrology……6

Methods……6

Hyrological and hydrochemical sampling……6

Identification of colloid content of water samples……8

Results and discussion……10

Hydrochemistry. ……10

Mineral stability diagram……12

Mixing model……13

Source of colloids……15

Conceptual model of colloid formation and movement in Gordon Gulch……19

Implications for soil development……23

Conclusion……23

References……25

Appendix A: Soil water data……29

Appendix B: Centrifuged surface and groundwater data……31

Tables

Table 1. Model comparison parameters for linear and power law fits of Al(/colloids) vs % Bedrock water (Figure 5)……..15

Table A1. Soil water data……29

Table B1. Centrifuged stream and groundwater data……31

Figures

Figure 1. Map of Gordon Gulch…… 4

Figure 2. Aluminum versus silica concentrations…… 9

Figure 3. Hydrochemistry time series…… 10

Figure 4. Mineral stability diagram…… 12

Figure 5. Al(/colloids) vs % bedrock water……14

Figure 6. Al(/colloids) and Cl^- time series……17

Figure 7. Conceptual diagram of colloid processes…… 18

Figure A1. Map of zero tension lysimeters in Gordon Gulch…… 29

Introduction

In environmental systems, inorganic colloids—inorganic particles in the size range from 0.01-100μm that can stay suspended in solution—consist of clays, amorphous silica, mica, and oxides, and form from weathering or oxidation of authogenic material or dust (reviewed by DeNovio et al. 2004). Inorganic colloids are chemically active because of their high surface area to volume ratio and surface charge. They mediate chemical reactions and bind organic matter, microorganisms, and solutes while simultaneously experiencing chemical changes themselves as they grow or weather. They are also mobile in the critical zone and carry materials, such as contaminants and immobile elements, that would otherwise remain stationary. Because inorganic colloids respond to both their geochemical and hydrological environments, they provide a unique intersection between fields that focus on transfer of physical material and fields that focus on transformations and movement of chemical species. For example, colloids provide an intermediary between chemical and physical weathering, which are traditionally considered separate processes (Kim et al., 2018), can be used as hydrochemical tracers (Aguirre et al. 2017; Mills et al., 2017), and contribute to the development of clay-rich soil horizons (Calabrese et al., 2018; Quenard et al. 2011).

Although understanding inorganic colloid production and movement is relevant to several fields, including fields that directly impact human health (DeNovio et al., 2004), no framework exists relating colloid production and export to critical zone properties such as soil type or weathering history. Such a framework is necessary to predict the importance of inorganic colloids in diverse environmental systems. In order to develop such a framework, I need to investigate inorganic colloid sources in various catchments with diverse critical zone properties. Here I develop a method of rapidly investigating colloid sources and export in a granitoid headwater catchment and employ it to predict where colloids are produced in its weathering profile.

While the literature on source locations of colloidal material in the critical zone is sparse, colloid movement through porous media is well defined in idealized conditions and has been studied in field cores and field sites. Colloid movement in saturated porous media can largely be described with the advection-dispersion equation but additions are needed to describe unsaturated conditions (Wan and Tokunaga, 1997; Bradford et al., 2003; DeNovio et al., 2004). Numerous laboratory experiments on idealized media or field samples have furthered our understanding of how colloid movement is affected by colloid composition, fluid ionic strength, dissolved organic matter, and redox conditions (e.g. Kretzchmar et al., 1997; Grolimund et al., 1998; Akbour et al., 2002; Sequaris et al., 2013; Kotch et al., 2016). Field studies have related colloid movement to hydrological and hydrochemical conditions (Zhang et al. 2015; Trostle et al., 2016; Zhang et al. 2016). However, while these models describe colloid movement, they do not predict colloid formation or export.

In soil, formation of the clay rich B-horizion has been attributed to downward migration of clay particles, including colloids, out of the E-horizon in a process called lessivage or argilluviation (reviewed by Quenard et al., 2011). Clay colloid translocation can be quantified by elements traditionally used as immobile indices in soil, such as Zr and Ti, which bind to clays and move with them (Bern et al., 2011). Recently, lessivage has been successfully modeled on long time-scales using a stochastic event-based approach (Calabrese et al., 2018).

I investigate where inorganic colloids are produced in a catchment where critical zone structure is well documented and inorganic colloids are important components of stream water and material efflux from the catchment. Gordon Gulch, a headwater catchment in the ephemeral snow zone of the Colorado Front Range, is part of the Boulder Creek Critical Zone Observatory (BcCZO). BcCZO staff and investigators have performed nearly a decade of hydrochemistry monitoring and numerous studies of critical zone structure in Gordon Gulch (e.g. Befus et al., 2011; Hinckley et al., 2012; Anderson et al., in prep). Efflux of inorganic colloids to stream water in Gordon Gulch represent about 37% of silica flux

from the catchment (Aguirre et al., 2017; Mills et al., 2017). Understanding colloid production and movement in this region is particularly important due to its history of mining (Dethier et al., 2018) and potential for colloids to facilitate contaminant transport. Additionally, inorganic colloid export is tied to hydrologic conditions in Gordon Gulch (Mills et al., 2017; Aguirre et al., 2017). Developing hydrologic models of catchments in the ephemeral snow zone is needed, as climate change is predicted to shift its meteorological forcings (Kampf and Lefsky, 2015), and this zone provides drinking water, affects water quality, and is understudied compared to the alpine (Hinckley et al., 2012).

Mills et al. (2017) identified colloids as an important component of silica flux in Gordon Gulch's stream water and observed colloidal kaolinite, illite, and amorphous Fe-hydroxides in stream water and soil leachate. However, they did not observe inorganic colloids in groundwater or, relatedly, in stream water during baseflow. Aguirre et al. (2017) confirmed that dissolved Si comes largely from groundwater and colloidal Si comes largely from shallower flow paths and found that this produces positive or near-zero power law slopes in concentration discharge relationships of total Si, Fe, and Al (dissolved and colloidal). Using Ge/Si ratios they identified incongruent weathering of feldspar as the main source of dissolved Si in groundwater and congruent weathering as the main source of colloidal Si.

I build on Mills et al. (2017) and Aguirre et al. (2017)'s studies by investigating what depth in Gordon Gulch's weathering profile produces inorganic colloids. I investigate inorganic colloid sources to stream water by developing a two-component mixing model of waters from different depths in the weathering profile and comparing it to a hydrochemical proxy for colloidal abundance in my long-term dataset. Mixing models are a widely used, easy to employ tool in catchment hydrology (Christophersen and Hooper, 1992). Mixing model component chemistry is often assumed to capture relevant hydrochemical processes. However, in my case I find it useful to develop a process-explicit model. I develop my mixing model in mineral stability space. My component chemistries are derived from two groundwater wells in Gordon Gulch, one screened in bedrock and one screened partially in bedrock and partially in saprolite

(used here to mean all material between mobile regolith and un-weathered rock). Using mineral stability allows us to comment on the potential for inorganic colloids to form in these two waters. I hypothesize that inorganic colloids are sourced from shallow depths in the weathering profile based on Mills et al. (2017) and Aguirre et al. (2017)'s findings. I then use the insight gained from analysis of colloids in stream water and their sources to develop a conceptual model of where colloids are produced and how they are transported through the critical zone in Gordon gulch.

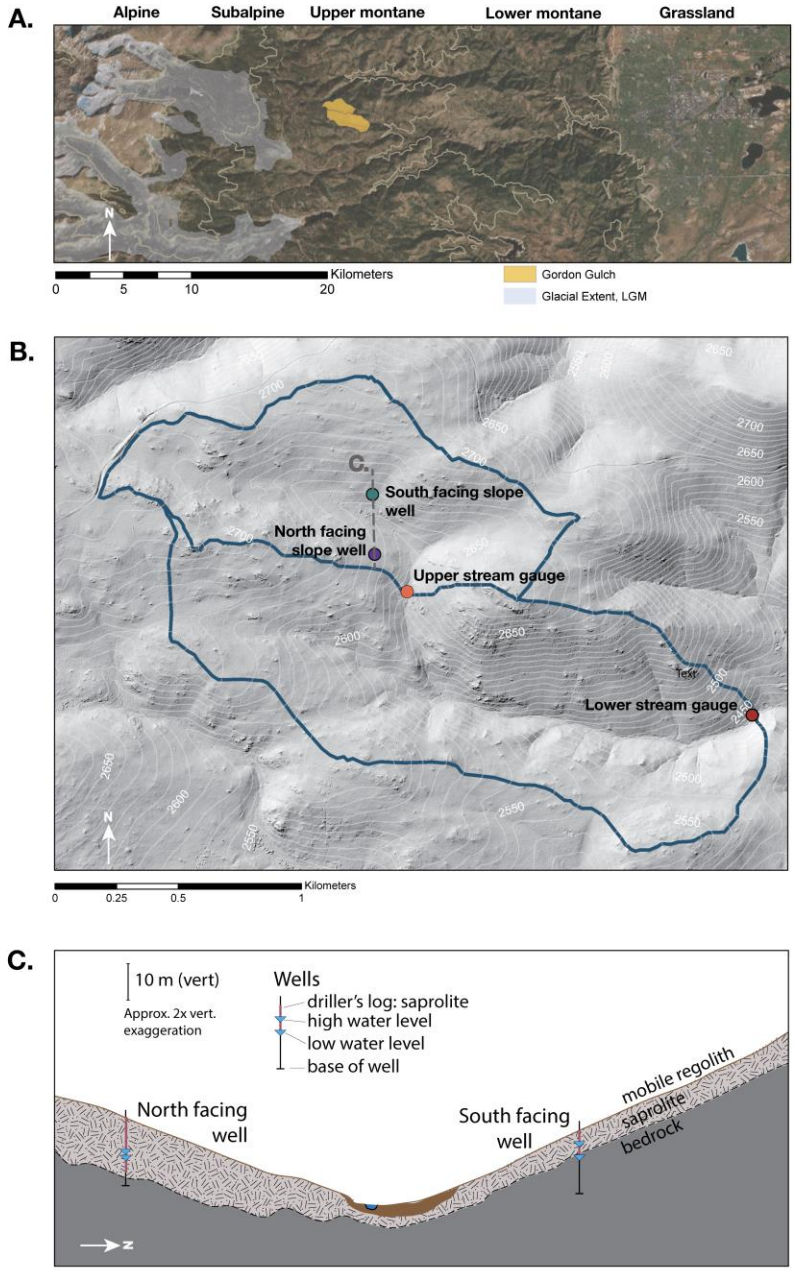

Figure 1. (A) East slope of Colorado Front Range from continental divide to Boulder, CO. (B) Hydrological sampling sites in Gordon Gulch including upper and lower Gordon Gulch stream gauges and north and south facing slope wells. (C) Cross section of upper Gordon Gulch including to-scale diagram of groundwater wells (modified with permission from Anderson et al, in prep).

Field site

Gordon Gulch is a 2.7km^2 headwater catchment at 2440-2730m elevation, midway between the plains of the Colorado plateau and the crest of the Colorado Front Range in the Rocky Mountains (Hinckley et al. 2012). Gordon Gulch is the mid-elevation study site of the Boulder Creek Critical Zone Observatory and has been monitored since mid-2008. In this catchment the bedrock, an 1800 Ma biotite gneiss pluton (Cole and Braddock, 2009), is overlain by 8-14m thick saprolite and ~40cm thick soil (Anderson et al., in review). Here I use "saprolite" to indicate all material between mobile regolith and un-weathered rock. I use "soil" and "mobile regolith" equivalently.

GG runs mainly east west (Figure 1). The north-facing slope is dominated by lodgepole pine (*Pinus contorta*) forest and retains a snowpack throughout winter and early spring (Hinckley et al., 2012; Langston et al., 2015). The south-facing slope is dominated by shrubs and grasses with scattered ponderosa pine (*Pinus Ponderosa*) and rapidly dissipates snow and rainwater through melt and evaporation. North facing slope saprolite is up to 2m thicker than south facing slope saprolite (Befus et al., 2011). Though differences in soil depth haven't been observed between slopes, the top 1-1.5m of saprolite are mechanically weaker on the north facing slope (Kelly, 2012; Anderson et al., 2014; Anderson et al., in revision). Soil on both slopes is designated Bulwark–Catamount families– Rubble land complex (USDA, 2016). The riparian zone contains willows and sub-alpine riparian vegetation. A grassy meadow lies in the center of the upper portion of the catchment. In addition to moisture, fire is a strong ecological driver in this catchment, reinforcing forest, riparian zone, and meadow composition (Veblen et al., 2000). Dust may be an important source of soil material in this catchment (Muhs and Benedict, 2006; Lawrence et al., 2013, Heindel et al., 2018).

Climate change is projected to aridify the catchment and reduce snowfall (Clow, 2010; Hale, 2018) causing fires to occur more often (Veblen et al., 2000). Over the last ~150 years, human use of the region has changed from use by the Núu-agha-tʉvʉ-pʉ (Ute) and Cheyenne Tribes, to mining, tree

removal, and heavy hunting by white settlers, to current recreation and scientific uses. Recreation and human caused fire is projected to continue increasing in the region for the foreseeable future, having impacts on soil forming processes such as ecological fragmentation and soil compression and erosion.

Field site hydrology

Typically, Gordon Gulch is most hydrologically active during spring, when snowmelt and precipitation are commonly at seasonal maxima. Peak meltwater stream flow is hydrochemically dominated by dilute water (Mills, 2016; Cowie et al., 2017; Zhang et al., 2018). Burns et al. (2007)'s analysis of organic matter movement through the catchment found evidence of near-surface water contribution to peak flow. Peak meltwater flow is preceded by a smaller peak in flow in March.

Summer low flows are sourced largely from groundwater and are concentrated with respect to weathering produced solutes (Mills, 2016; Aguirre et al., 2017; Mills et al., 2017; Cowie et al., 2017; Zhang et al., 2018). In fall evapoconcentrated depositional solutes such as chloride and sulfate are flushed out of soils (Mills, 2016). Winter flows are low and moderately concentrated (Mills, 2016).

Fractures are observed in Gordon Gulch's weathering profile (St. Clair et al., 2015) and may provide conduits through the critical zone (Appendix 4). Macropore flow is more important in soils on the south facing slope than the north facing slope (Hinckley et al., 2012, 2014, 2017).

Methods

Hydrological and hydrochemical sampling

I utilize long-term hydrological and hydrochemical records from the BcCZO. Gordon Gulch is split into two sections, upper Gordon Gulch and lower Gordon Gulch (Figure 1). Stream water was sampled once per week at the outlets of upper and lower Gordon Gulch. Discharge was measured using the salt

dilution method (Kite, 1993; Hongve, 1987) about once a week. I developed a rating curve using data from a Solinst Gold pressure transducer maintained by BcCZO staff to compute a discharge record between manual measurements. One discharge event was excluded on May 9, 2015, as transducer data appears unreliable during this period. Rating curve fit is strong for water years 2015-2018 but is less reliable for water year 2014. Two groundwater wells in the upper basin were monitored with a pressure transducer (Solinst Gold Level Logger) for water level and were sampled about once per month (Figure 1). Well 1, on the north-facing slope, is 18.55 m deep, and screened 9.41 m below the surface, 56% in saprolite and 43% in bedrock. Well 6, on the south-facing slope, is 17.34 m deep, and screened at 8.2 m below the surface, and 100% in bedrock. (Wells 2-5, located in the riparian area, are not used in this study.)

All water samples were collected and processed by staff of the Boulder Creek Critical Zone Observatory and analyzed as described in Mills et al. (2017). Briefly, water samples were stored at 4°C and filtered through 0.45 micron filters within 72 hours. Samples were analyzed for major cations, Si, Fe, and Al with inductively coupled plasma optical emission spectroscopy (ICP–OES) at the Laboratory for Environmental and Geological Sciences in Boulder, CO. Samples were analyzed for major anions with ion chromatography at the Boulder Creek CZO laboratory. Prior studies of inorganic colloids in Gordon Gulch have quantified colloidal abundance by comparing filtered samples that contain both colloidal and dissolved material to filtered samples where colloidal material has been removed through centrifugation (Mills et al., 2017; Aguirre et al., 2017). In this study I use total Al concentration as a proxy for colloidal abundance as described below.

Weekly precipitation was measured by the National Atmospheric Deposition Program at the Sugarloaf Mountain Station (CO94), 2.8km away (NADP, 2019).

Identification of colloid content of water samples

My dataset comprises stream and groundwater chemistry from the BcCZO's long-term hydrochemistry monitoring dataset. The BcCZO does not monitor colloid concentrations so I develop a proxy for inorganic colloid abundance in BcCZO monitoring data based on observations by Aguirre et al. (2017) and Mills et al. (2017).

Aguirre et al. (2017) and Mills et al. (2017) found inorganic colloids in Gordon Gulch stream water consisting of kaolinite, illite, oxides, and amorphous silica, and composed primarily of Si, Al, and Fe. I focus on Al and Si concentrations in stream and groundwater because they have been monitored continuously by the BcCZO during my study period, 2014-2018. The BcCZO measures total Al and Si, including dissolved and colloidal fractions, with ICP-OES in samples filtered through a 0.45 micron filter. Aguirre et al. (2017) and Mills et al. (2017) measured colloid concentrations by finding the difference in elemental composition between filtered samples, which include colloids, and samples where they removed colloids by centrifugation, leaving the dissolved fraction. I infer that Al is entirely in colloidal form in BcCZO samples because Aguirre et al. (2017) and Mills et al. (2017) found Al only in colloidal form and Al is highly insoluble in circum-neutral water. On the other hand, total Si concentrations include both dissolved and colloidal Si (Aguirre et al., 2017; Mills et al., 2017). Colloidal Si varies seasonally whereas concentrations of dissolved Si are relatively constant (Aguirre et al., 2017; Mills et al., 2017).

Aguirre et al. (2017) found a strong linear correlation between total Al concentration and total Si concentration in BcCZO stream water samples. They found that the slope of the relationship between Al and Si concentrations was equal to the ratio between Al and Si elemental compositions in inorganic colloids. I infer from Aguirre et al. (2017)'s finding that both Al and Si total concentrations could be used as a proxy for inorganic colloid abundance in Gordon Gulch.

I choose to use total Al concentrations over total Si concentrations as a proxy because Al is likely present only in colloidal form in BcCZO samples, whereas Si is likely present in both colloidal and dissolved form—variation in dissolved Si concentration would change my estimation of colloidal abundance. I infer that total Al concentration represents total colloid abundance (as opposed to abundance of colloids with Al as the primary cation, e.g. gibbsite) because the slope of the fit between Al and Si concentrations corresponded to total inorganic colloid composition.

To ensure that Al is a valid proxy for colloid abundance during my study period, I plot Al concentrations against Si concentrations in non-centrifuged stream water samples from the BcCZO's long-term monitoring program from 2014 to 2018 (Figure 2). I find several high Si outliers and address them by using a Least Absolute Deviation linear fit. My findings replicate Aguirre et al. (2017)'s strong linear relationship between Al and Si. My slopes were within 0.08 of Aguirre et al. (2017), with pseudo R^2 of 0.28 for lower Gordon Gulch and 0.58 for upper Gordon Gulch, and P-Values of <0.001.

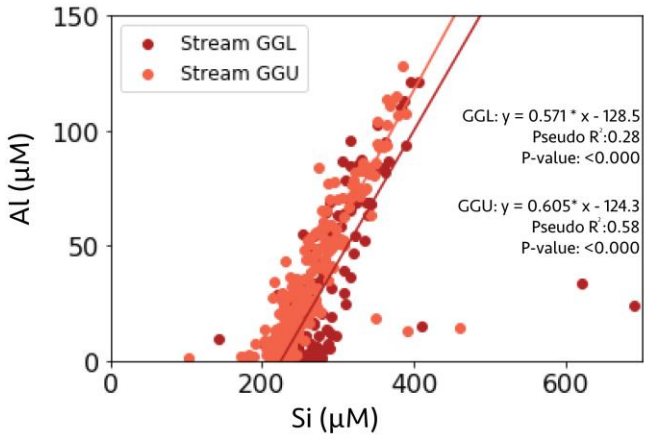

Figure 2. Aluminum versus silica concentrations analyzed by ICP-OES in stream water at the lower Gordon Gulch (GGL) and upper Gordon Gulch (GGU) guages. Linear Absolute Derivation used for linear fit to minimize influence of outliers.

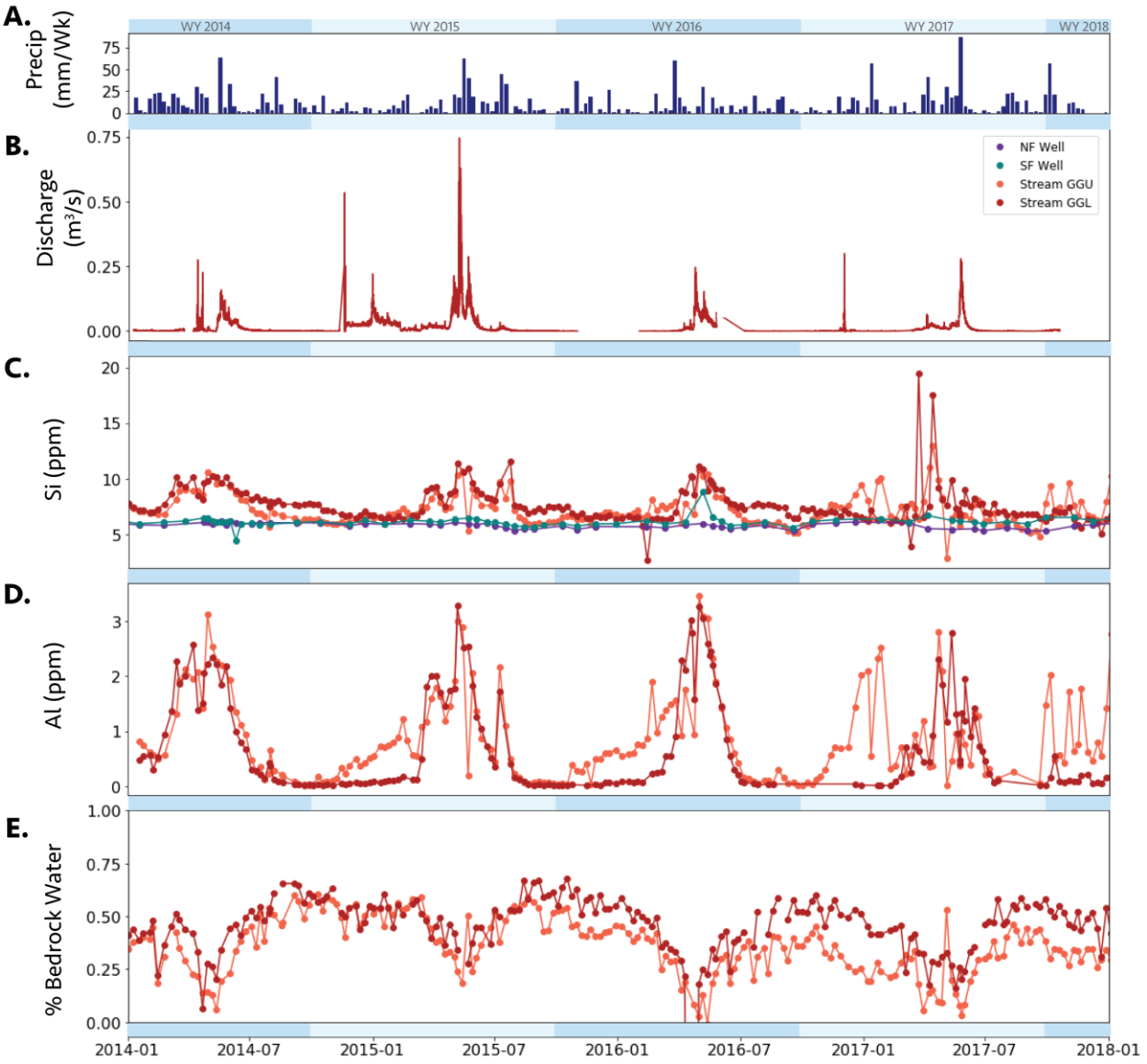

Figure 3. (A) Weekly precipitation at the NADP Sugarloaf site, 2km from Gordon Gulch (NADP, 2019). (B) Discharge at lower Gordon Gulch gauge (GGL). (C) Si concentrations at lower and upper Gordon Gulch gauges (GGL and GGU respectively) and north and south facing slope wells (NF and SF, respectively). Both dissolved and colloidal silica are present. (D) Al concentrations at GGL and GGU. Al was below detection in all but two samples (not shown) in the north and south facing slope wells. For reasons outlined in the text, Al concentrations are used to represent inorganic colloid abundance. (E) Results of mixing model between "saprolite" and "bedrock" water.

Results and discussion

Hydrochemistry

Here I describe seasonal trends in inorganic colloid abundance and hydrochemistry to enable comparison with my saprolite/bedrock-explicit mixing model, which I develop below. Average annual

precipitation from 2014 to 2018 at the NADP Sugarloaf weather station near Gordon Gulch was 53 cm (NADP, 2019). Seasonally, Al(/colloids) peak in stream water during snowmelt, decline during the falling limb, and are absent during late summer and early fall (Figure 3D). They re-appear in upper Gordon Gulch stream water in mid-fall and re-appear in lower Gordon Gulch stream water only during snowmelt. Al(/colloids) are not found in groundwater (note low Si in Figure 3C), with the exception of two points during the snowmelt peak of 2016 in which the south-facing slope well had elevated aluminum (not shown).

Total Si concentration peaks in stream water during the main spring snowmelt discharge peak. Total Si concentrations drop to ~6 ppm during late summer low flow while Al(/colloid) concentrations drop to zero. This silica concentration minimum is likely in dissolved form and has been attributed to groundwater effluence (Aguirre et al., 2017; Mills et al., 2017). Groundwater silica concentrations are relatively dilute and stable compared to stream water. This is likely due to absence of colloidal silica, as instances of stream water silica concentrations rising above groundwater concentrations coincide with peaks in stream water Al(/colloid) concentrations.

Groundwater concentrations of silica rise slightly during peak snowmelt discharge, especially in the south facing well in 2016 (Figure 3). Increased groundwater total silica concentrations during peak flow are likely due to an influx of silica from shallower, younger, more aggressive water that is exposed to easily weathered rock as it moves down through the weathering profile. Anderson et al (in prep) attributed groundwater table rise during peak snowmelt flow to an influx of meltwater.

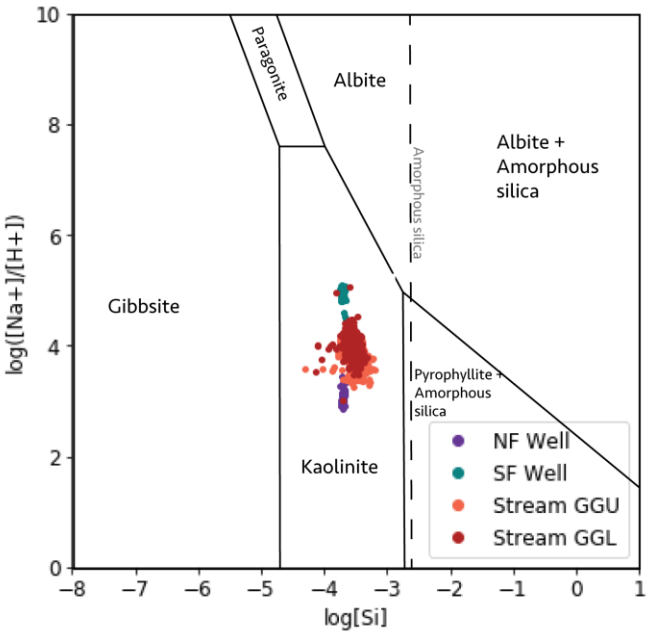

Figure 4. Mineral stability diagram including stream water chemistry at upper and lower Gordon Gulch (GGU and GGL respectively) and groundwater chemistry from north- and south- facing wells (NF Well and SF Well respectively).

Mineral stability diagram

I plot the compositions of stream water and of north- and south- facing well water on mineral stability diagrams to investigate the thermodynamic stability of secondary minerals, which form inorganic colloids in this catchment, in these different waters (Fuare, 1998). This method is useful because it gives us insight into the boundary conditions affecting water-rock interactions, however, this method does not allow us to comment on dissolution and precipitation kinetics or the influence of organic matter or microorganisms on weathering.

I examined mineral stability diagrams for systems involving Ca^{2+}, Na^{+}, K^{+}, H_2O, Al_2O_3 and Si, but show only the Na^{+}-Si-H_2O system in Figure 4. Plotted in this way, water chemistry of the stream and each well separate into distinct compositional spaces. North-facing well water lies entirely in the kaolinite mineral stability space. South-facing well water lies mostly in the kaolinite mineral stability space but is, at times, in equilibrium with illite, muscovite, or calcite (later relationships not shown). Stream water is contained

entirely in the kaolinite stability field, and is bounded along the y-axis by water from the north- and south- facing wells. While there is noticeable variation along the y-axis, variation on the x-axis is negligible.

Mixing model

On the mineral stability diagram (Figure 4) stream water is constrained by the compositions of the north- and south-facing wells. Because stream water is constrained by the north- and south-facing wells on the mineral stability diagram, I can build a mixing model for stream water between the two wells that gives us insight into what depth in the weathering profile stream water is coming from. I interpret north-facing well water as characteristic of saprolite because the well is screened partially in saprolite, is more dilute than the south-facing well, and is consistently in the kaolinite stability field. I infer south facing well water to be bedrock water because it is screened entirely in bedrock, is more concentrated, and is farther into the "rock dominated" portion (i.e., near the albite stability field) of the mineral stability diagram. I follow the two component mixing model form:

$$\frac{Volume\ of\ interest}{Total\ volume} = \frac{(Total\ concentration - Concentration\ 1)}{(Concentration\ 2 - Concentration\ 1)}$$

I use stream water chemistry as "total concentration", north facing well chemistry as "Concentration 1," and south facing well chemistry as "Concentration 2."

Through the mixing model I find that stream water varies between ~0 and ~60% bedrock water and stream water is never composed entirely of bedrock water (Figure 3). Peak snowmelt is dominated by saprolite water and baseflow is a mix of saprolite and bedrock water. The mixing model shows a different aspect of stream water production than previous mixing models in the catchment, which focused on type of water source (e.g. precipitation, groundwater) rather than spatial location of water source (Mills, 2016; Cowie et al., 2017). However, my models align with previous mixing models in that

dilute endmembers dominate during spring snowmelt and concentrated endmembers dominate during low-flow (Mills, 2016; Cowie et al., 2017).

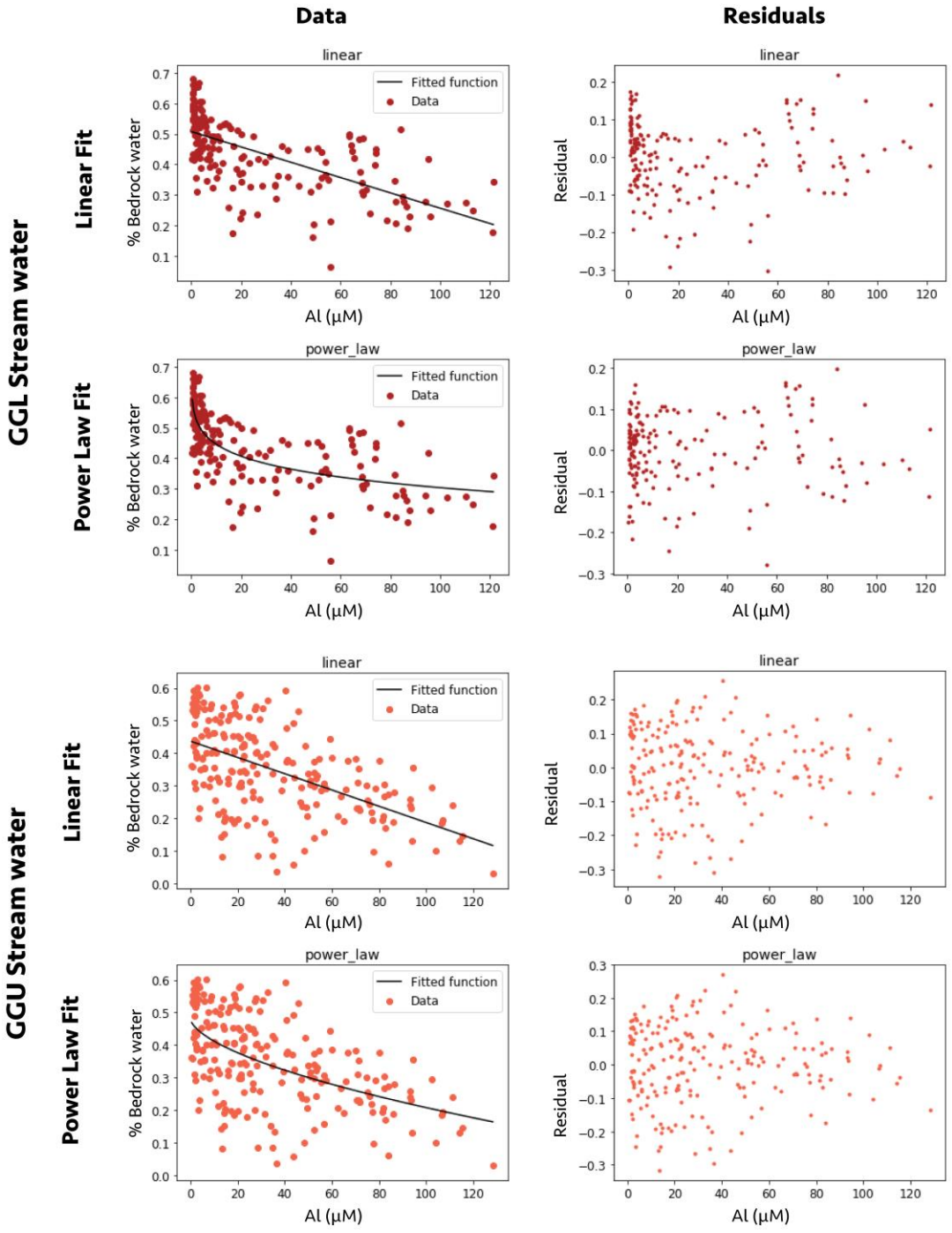

Figure 5. Al(/colloids) vs % bedrock water in lower and upper Gordon Gulch (GGU and GGL). Black lines are modeled linear and power law fits, plots on the right are their residuals. Linear fit based on: $y = m*x + b$; Power law fit based on: $y = m * x^c + b$.

Table 1. Model comparison parameters for linear and power law fits of Al(/colloids) vs % Bedrock water (Figure 5).

Lower Gordon Gulch				
Model:	**AICc**	**R^2**	**Delta**	**Evidence Ratio**
Linear	-848.27	0.41	31.66	$7.5 * 10^6$
Power Law	-879.93	0.51	0	1
Upper Gordon Gulch				
Model:	**AICc**	**R^2**	**Delta**	**Evidence Ratio**
Linear	-925.91	0.30	0.6246	1.367
Power Law	-926.53	0.31	0	1

Source of colloids

I can now use the stream water colloid proxy and the mixing model to elucidate colloid sources in the Gordon Gulch. I find that %bedrock water and Al(/colloids) co-vary (Figure 5). Al(/colloid) concentrations are inversely related to percent bedrock water, indicating that colloidal fluxes in stream water are elevated when efflux of saprolite water is high. I found that a linear regression model moderately to poorly describes the relationship between Al(/colloids) concentrations and % Bedrock water (R^2_{GGL}: 0.41, R^2_{GGU}: 0.30 ; P-value $_{GGL}$ < 0.001, P-value $_{GGU}$ <0.001). However, while R^2 values are moderate to poor, P-values are low, indicating that the relationship is not random.

Although I do not have a theoretical basis to perform a non-linear regression at this time, I investigate the utility of a non-linear relationship by performing a sample non-linear regression. I choose a power-law model ($y = m*x^c + b$) for simplicity and fit it using the Python package Scipy. I find that a power law regression substantially out-performs a linear regression for lower Gordon Gulch but not for upper Gordon Gulch (Table 1).

Statistics used to compare statistical models include the corrected Akaike Information Criterion (AICc), delta values, and evidence ratios. AICc is a measure of relative performance between models where a lower value means better performance. The delta is the difference between AICc values for different models of the same dataset—a value greater than two is considered enough to disqualify a model (Burnham and Anderson, 2002). The evidence ratio is a measure of how much evidence there is that one

model is outperformed by another. The power law regression of lower Gordon Gulch has a lower AICc than my linear regression; the delta value of the linear regression is substantially over two; and there is $7.5 * 10^6$ more evidence that the power law regression out-performs the linear regression (Table 1). In upper Gordon Gulch none of these statistics show that either model out-performs the other by a meaningful amount. Regardless, the correlation between Al(/colloid) abundance with flow from saprolite is clear.

I observe that Al(/colloid) concentrations in upper Gordon Gulch stream water diverge from lower Gordon Gulch stream water annually in the fall but are otherwise quite similar (Figure 6). The reason for this divergence is not clear, though I observe that it begins at the same time as spikes of Cl^- in stream water, especially in upper Gordon Gulch, in WY 2015 and WY 2016 (Figure 6), drops in weathering produced solutes (e.g. Na^+, Ca^{2+}) in upper Gordon Gulch relative to lower Gordon Gulch (not shown), and dilution towards my saprolite component in the mixing model in upper Gordon Gulch (Figure 3).

The correlation between Al(/colloids) and saprolite water in Gordon Gulch stream water indicates that inorganic colloids are sourced from saprolite. Saprolite water is most prevalent during high spring flows, corresponding to peaks in Al(/colloids). Bedrock water is most prevalent at low flow when Al(/colloids) are absent in lower Gordon Gulch and at low concentrations in upper Gordon Gulch. Stream water varies between ~0 and ~60% bedrock water. The relationship between Al(/colloid) concentrations and %bedrock water is non-linear, however, more work is needed to develop a theoretical basis for this relationship. Colloidal material is rarely observed in either well. I hypothesize that colloids do come from saprolite but are available for export to stream water from shallower in saprolite where more dilute water is capable of entraining colloid material.

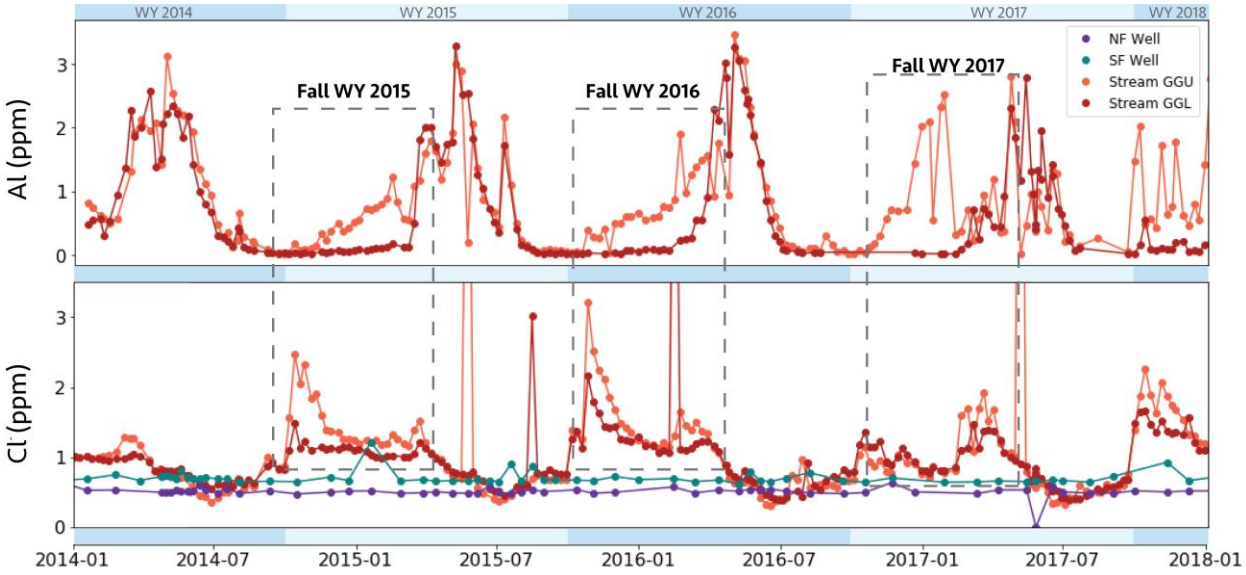

Figure 6. Time series of Al(/colloids) and Cl^- concentrations in lower and upper Gordon Gulch stream water (GGL and GGU) and in the north and south facing wells (NF Well and SF Well). Dashed boxes indicate times when Al(/colloid) concentrations in GGU diverge from Al(/colloid) concentrations in GGL. In WY 2016 and WY 2016 this corresponds with elevated in Cl^- concentration.

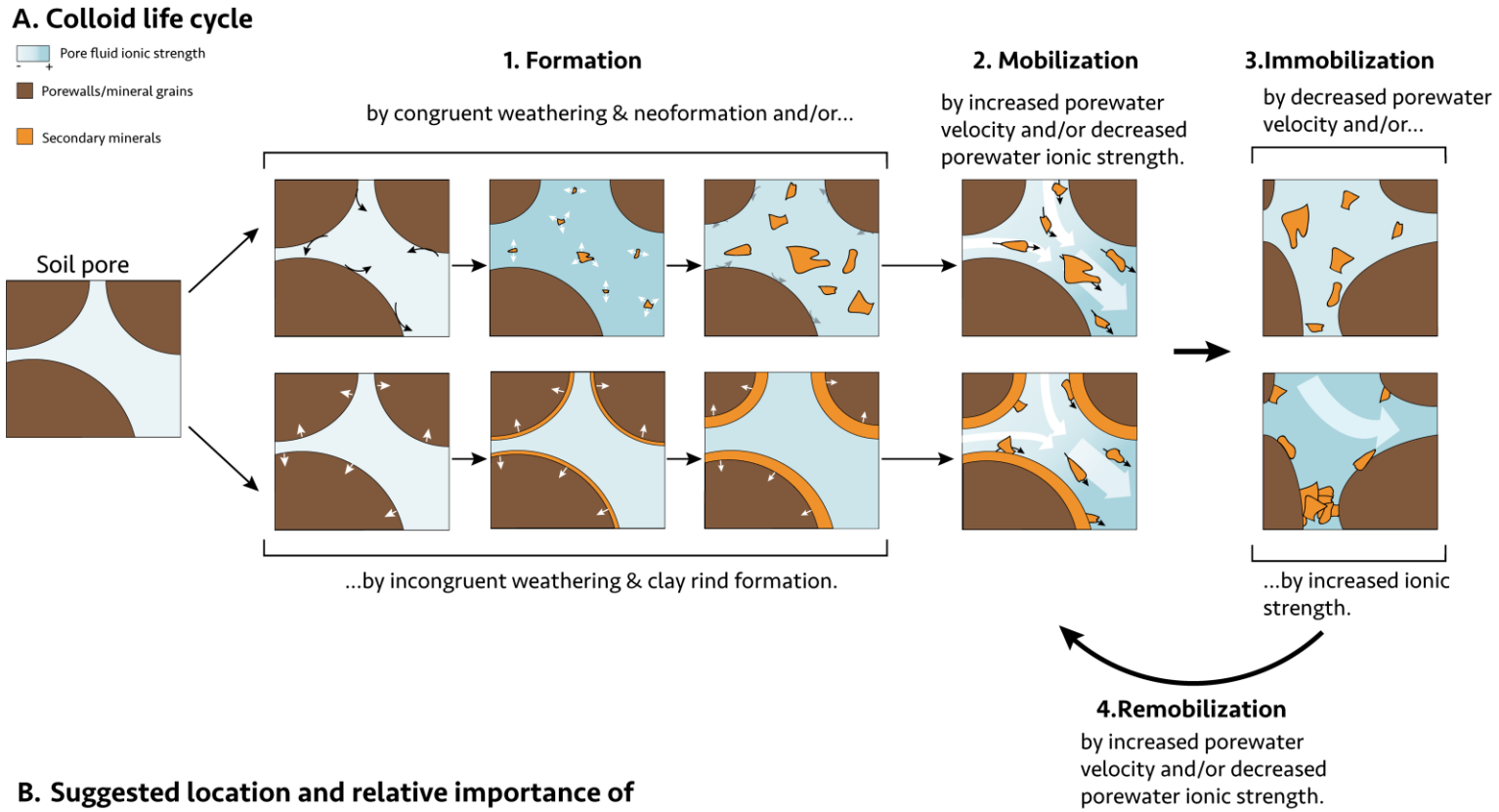

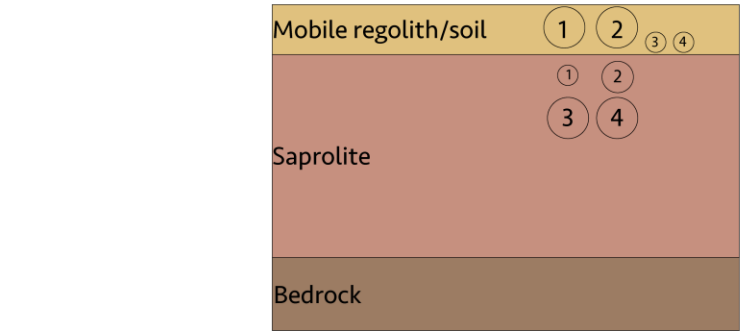

Figure 7. A. Depiction of colloid formation (1), mobilization (2), immobilization (3), and remobilization (4) in soil pores. B. Hypothesized location of colloid processes. Numbers correspond to numbers of processes depicted in A.

Conceptual model of colloid formation and movement in Gordon Gulch

Based on my finding that inorganic colloids get entrained into Gordon Gulch's hydrologic system in saprolite and prior work in the catchment, I propose a mechanism whereby inorganic colloidal material is produced, recycled, and exported. I describe a general conceptual model and then describe how it applies to Gordon Gulch.

General conceptual model (Figure 7A):

1. Secondary mineral formation and colloid production from secondary minerals: Primary minerals are dissolved where young, chemically aggressive water weathers available mineral surfaces. Organic acids and microorganisms can increase or decrease mineral weathering rates depending on the environment.

   Secondary minerals, which make up inorganic colloids in this catchment, may be formed in place on the surface of mineral grains (incongruent weathering) or through neoformation, where-in they precipitate out of solution (congruent weathering and precipitation). Neoformation can occur on the surface of pore walls or suspended in solution, and is often nucleated. Suspended particles are considered colloidal below ~100 microns; we consider small colloids below 0.45 microns. Before neoformation occurs, ions may travel away from the site of primary mineral dissolution before re-precipitating. Secondary minerals can also be deposited as dust or originate from bedrock.
2. Colloid mobilization: Colloids suspended in solution are translocated when porewater moves. Additionally, colloid sized particles can be ripped from secondary mineral coatings on pore walls when pore water physically scours particles from walls or when an influx of lower ionic strength water releases grains. Colloids are then translocated deeper into the weathering profile and/or downslope.

3. Colloid immobilization: Colloids are immobilized when the water carrying them stops moving, when they are captured by microbial biofilms, or when they exposed to higher ionic strength water, which causes them to flocculate to themselves and pore walls.
4. Colloid remobilization: Colloids are remobilized when pore water moves, when pore water physically scours secondary coatings, and/or when lower ionic strength pore water is introduced.

Location of colloid processes in Gordon Gulch (Figure 7B):

1. Formation of secondary minerals and colloids: Aguirre et al. (2017) found that colloids are likely formed by incongruent weathering in saprolite or mobile regolith based on Ge/Si values. Dust deposition is likely an important source of secondary minerals in this catchment (Heindel et al., in prep) and has been found to play a major role in soil formation in the region (Muhs and Benedict, 2006; Lawrence et al., 2013). Additionally, kaolinite has been found in Gordon Gulch's bedrock from hydrothermal alteration (Gable et al., 1996). Secondary minerals were found sporadically up to 14m in coring chips (Eldam, 2016).

   I predict that secondary mineral formation from weathering likely happens proportionally more in mobile regolith than in saprolite because grains are much smaller than in saprolite, providing a higher surface area to volume ratio, and water is younger and more chemically aggressive. Weatherable material is likely more available in Gordon Gulch's poorly developed soil than in a more developed soil, as the mobile regolith has a low index of chemical alteration (Eldam, 2016), low weight percent clay (Anderson et al., in review), and low organic matter content (Gabor et al., 2014). Additionally, physical weathering dominates in this catchment (Anderson et al., in review), indicating that a higher proportion of surfaces are less chemically altered—and therefore available for chemical weathering—than in a catchment where chemical weathering dominates.

2. Colloid mobilization and immobilization: I predict that colloids are formed predominantly in mobile regolith and upper saprolite then translocated deeper into saprolite and exported to the stream. Foster et al. (2015) found meteoric ^{10}Be, which enters the critical zone in rain, deeper in saprolite than expected. ^{10}Be is known to bind to clays that have been found in colloidal fraction in this catchment, such as illite (the binding of ^{10}Be to clays forms the basis of meteoric ^{10}Be work in geochronology and geomorphology) (e.g. Boschi and Willenbring, 2016). Therefore, the presence of ^{10}Be in saprolite may reflect movement of inorganic colloids from shallow in the critical zone to saprolite and subsequent storage of colloidal material in saprolite. Foster et al. (2015) hypothesized that meteoric ^{10}Be is brought to saprolite by rapid infiltration of meteoric water, however, their study was published before it was known that colloidal material is prevalent in Gordon Gulch (Mills, 2016).)

   I predict that inorganic colloids are immobilized in Gordon Gulch's critical zone chiefly due to increases in pore water ionic strength with depth. Previous work attributed the lack of inorganic colloids in Gordon Gulch's groundwater to high ionic strength, which causes colloids to flocculate to walls and each other (Mills et al., 2017; Degueldre et al., 1996). This is supported by Degueldre et al. (1996), who found that high ionic strength caused colloids to be absent from groundwater in a similar catchment. An alternative hypothesis for colloid immobilization is that colloids are strained by declining pore space and connectivity deeper in the weathering profile. However, Gordon Gulch's bedrock has been found to be fractured (St. Clair et al., 2015) and the groundwater table rises quickly in response to snowmelt (Anderson et al., in prep) so it is unlikely that water—and thus colloids—meet substantial pore-scale barriers (on average across the catchment).

   In Gordon Gulch clays and oxides have been found as deep as 8m (Eldam, 2016). In a nearby lower elevation catchment also studied by the BcCZO clay rinds on pore walls have been found

in saprolite (Anderson et al., 2013). Gordon Gulch's bedrock is relatively heterogenous (Eldam 2016) so zones of inorganic colloid formation, mobilization, and immobilization/storage are likely mosaicked across the landscape.

3. Sources of inorganic colloids to stream water: I find that inorganic colloids in stream water are sourced from saprolite or mobile regolith and that secondary minerals are stable in both stream and groundwater. My observations replicate the results of Mills et al. (2017)—in this catchment stream water colloid concentrations are the highest during high melt water flows, sourced from shallow water, and lowest during predicted baseflow, sourced from mixed groundwater-shallow water.

   I predict that colloids are exported to the stream from mid- to upper-saprolite. On the upper bound, the negative relationship I observe between Al(/colloids) and chloride concentrations in upper Gordon Gulch in fall may indicate that inorganic colloids are sourced from below mobile regolith, as chloride is entirely depositional in Gordon Gulch and becomes evapoconcentrated in mobile regolith (described by Mills, 2016). On the lower bound, inorganic colloids are not found in groundwater, including in the north facing well, which I use as my "saprolite" end member. Because ionic strength is likely the primary culprit immobilizing colloids, colloids are likely carried out of saprolite by more dilute, shallower water than is seen in the north facing well. This is possible—though I use the north facing well as a representation of saprolite water, the north facing well is ~43% bedrock by depth and is therefore likely more concentrated than shallower water.

Implications for soil development

Inorganic colloid movement into saprolite has implications for soil formation because transfer of clays and oxides have been found to influence the development of soil layers (e.g. Calabrese et al., 2018). However, soil horizonation is weak in this catchment. I hypothesize that secondary mineral storage likely

occurs below mobile regolith. Therefore, clay movement is likely a separate, deeper process than soil horizonation in this catchment.

Over long timescales it is possible that parcels of clay in saprolite lower as the surface of mobile regolith lowers, carried by fresh water permeating into the critical zone. Production and movement of clay parcels would be disrupted by changes in ionic strength of permeating water and changes in rate and timing of hydrologic fluxes. If clay parcel movement in saprolite is disturbed (e.g. by climate changes), clay rich parcels could be incorporated into mobile regolith and cause state change in local soil forming processes.

Conclusion

The goal of this study is to develop a lithogenic mixing model to understand where inorganic colloids originate in a catchment and how their export from the critical zone relates to seasonal hydrologic patterns. In this study I take advantage of the Boulder Creek Critical Zone Observatory's long term monitoring of Gordon Gulch, a montane catchment in the Colorado Front Range. I develop an endmember mixing model based on mineral stability. I find that stream water mineral stability is constrained between two groundwater wells in the catchment—one that is screened entirely in bedrock and one that is screened partially in bedrock and partially in saprolite. I then test my hypothesis that mineral stability and type of source material (bedrock vs saprolite) is related to colloidal abundance over time. I find that colloid efflux is positively related to amount of saprolite water. Based on my endmember mixing model younger saprolite water dominates streamflow during peak meltwater flow; inorganic colloids are most concentrated during this time.

My mixing model method could be useful predicting inorganic colloid location and efflux in other catchments underlain by metamorphic and igneous bedrock, which is useful to several fields. In soil development and geomorphology, my model could aid modeling of silicate translocation processes. In

contaminant transport, my model could aid understanding and predicting colloid movement through the subsurface. In hydrology, my model could aid fine-tune hydrologic models and make them hydrochemically process explicit.

Future work is needed to open the black box of inorganic colloidal processes in saprolite. Previous work on inorganic colloid processes has focused on mobile regolith (e.g. Bern et al., 2015). However, I find that saprolite is an integral location for inorganic colloid storage and movement in my catchment. Whereas mobile regolith is core-able and can be removed for laboratory experimentation, saprolite extraction requires drilling or a pre-existing road cut and is thereby difficult to investigate experimentally. Therefore I suggest a combined approach between numerical modeling, field observations, and experimentation.

National Atmospheric Deposition Program. (n.d.).

Aguirre, A. A., Derry, L. A., Mills, T. J., & Anderson, S. P. (2017). Colloidal transport in the Gordon Gulch catchment of the Boulder Creek CZO and its effect on C-Q relationships for silicon. *Water Resources Research*, *53*(3), 2368–2383. https://doi.org/10.1002/2016WR019730

Akbour, R. A., Douch, J., Hamdani, M., & Schmitz, P. (2002). Transport of Kaolinite Colloids through Quartz Sand: Influence of Humic Acid, Ca2+, and Trace Metals. *Journal of Colloid and Interface Science*, *253*(1), 1–8. https://doi.org/10.1006/jcis.2002.8523

Anderson, S. P., Hinckley, E.-L., Kelly, P., & Langston, A. (2014). Variation in Critical Zone Processes and Architecture across Slope Aspects. *Procedia Earth and Planetary Science*, *10*, 28–33. https://doi.org/10.1016/j.proeps.2014.08.006

Anderson, SP, Wlostowski, A, and Murphy, SF (In preparation): Hydrology in the transitional snow persistence zone: Runoff generation in a semi-arid basin. For *Hydrological Processes*.

Anderson, SP, Kelly, PJ, Hoffman, N, Barnhart, K, Befus, K, and Ouimet, W (In review): Is this steady state? Weathering and critical zone architecture in Gordon Gulch, Colorado Front Range. For *Chemical Weathering and Soil Formation*, AGU Water Resources Monograph, ed. by A.G. Hunt and M. Egli.

Bern, C. R., Chadwick, O. A., Hartshorn, A. S., Khomo, L. M., & Chorover, J. (2011). A mass-balance model to separate and quantify colloidal and solute redistributions in soil. *Chemical Geology*, *282*(3–4), 113–119. https://doi.org/10.1016/j.chemgeo.2011.01.014

Bern, C. R., Thompson, A., & Chadwick, O. A. (2015). Quantification of colloidal and aqueous element transfer in soils: The dual-phase mass balance model. *Geochimica et Cosmochimica Acta*, *151*, 1–18. https://doi.org/10.1016/j.gca.2014.12.008

Boschi, V., & Willenbring, J. K. (2016). Beryllium desorption from minerals and organic ligands over time. *Chemical Geology*, *439*, 52–58. https://doi.org/10.1016/j.chemgeo.2016.06.009

Burns, M. A., Barnard, H. R., Gabor, R. S., McKnight, D. M., & Brooks, P. D. (2016). Dissolved organic matter transport reflects hillslope to stream connectivity during snowmelt in a montane catchment. *Journal of the American Water Resources Association*, *52*(6), 4905–4923. https://doi.org/10.1002/2015WR017878

Calabrese, S., Richter, D. D., & Porporato, A. (2018). The Formation of Clay-Enriched Horizons by Lessivage. *Geophysical Research Letters*, *45*(15), 7588–7595. https://doi.org/10.1029/2018GL078778

Chirstophersen, N., & Hooper, R. (1992). Multivariate Analysis of Stream Water Chemical Data' The Use of Principal Components Analysis for the End-Member Mixing Problem. *Water Resources Research*, *28*(1), 99–107.

Clow, D. W. (2010). Changes in the timing of snowmelt and streamflow in Colorado: A response to recent warming. *Journal of Climate*, *23*(9), 2293–2306. https://doi.org/10.1175/2009JCLI2951.1

Cole, J. C., & Braddock, W. A. (2009). Geologic Map of the Estes Park 30 ' x 60 ' Quadrangle , North-Central Colorado. *US Geological Survey Scientific Investigations Map 3039*, *pamphlet*, 56 p.

Cowie, R. M., Knowles, J. F., Dailey, K. R., Williams, M. W., Mills, T. J., & Molotch, N. P. (2017). Sources of streamflow along a headwater catchment elevational gradient. *Journal of Hydrology*, *549*, 163–178. https://doi.org/10.1016/j.jhydrol.2017.03.044

Degueldre, C., Pfeiffer, H. R., Alexander, W., Wernli, B., & Bruetsch, R. (1996). Colloid properties in granitic groundwater systems. I: Sampling and characterisation. *Applied Geochemistry*, *11*(5), 677–695. https://doi.org/10.1016/S0883-2927(96)00036-4

DeNovio, N. M., Saiers, J. E., & Ryan, J. N. (2004). Colloid Movement in Unsaturated Porous Media: Recent Advances and Future Directions. *Vadose Zone Journal*, *3*(2), 338–351. https://doi.org/10.2113/3.2.338

Dethier, D. P., Birkeland, P. W., & McCarthy, J. A. (2012). Using the accumulation of CBD-extractable iron and clay content to estimate soil age on stable surfaces and nearby slopes, Front Range, Colorado. *Geomorphology*, *173–174*, 17–29. https://doi.org/10.1016/j.geomorph.2012.05.022

Dethier, D. P., Ouimet, W. B., Murphy, S. F., Kotikian, M., Wicherski, W., & Samuels, R. M. (2018). Anthropocene landscape change and the legacy of nineteenth- and twentieth-century mining in the fourmile catchment, Colorado front range. *Annals of the American Association of Geographers*, *108*(4), 917–937. https://doi.org/10.1080/24694452.2017.1406329

Eldam, R. (2016). Evaluating Control of Slope-Aspect on Geochemical Weathering Within the Boulder Creek Critical Zone Observatory. *Master's Thesis*. https://doi.org/10.1017/CBO9781107415324.004

Faure, G. (1998). *Principles and Applicaitons of Geochemistry* (2nd ed.). Prentice Hall.

Foster, M. A., Anderson, R. S., Wyshnytzky, C. E., Ouimet, W. B., & Dethier, D. P. (2015). Hillslope lowering rates and mobile-regolith residence times from in situ and meteoric10Be analysis, Boulder Creek Critical Zone Observatory, Colorado. *Bulletin of the Geological Society of America*, *127*(5–6), 862–878. https://doi.org/10.1130/B31115.1

Gabor, R. S., Eilers, K., McKnight, D. M., Fierer, N., & Anderson, S. P. (2014). From the litter layer to the saprolite: Chemical changes in water-soluble soil organic matter and their correlation to microbial community composition. *Soil Biology and Biochemistry*, *68*, 166–176. https://doi.org/10.1016/j.soilbio.2013.09.029

Grolimund, D., Elimelech, M., Borkovec, M., Barmettler, K., Kretzschmar, R., & Sticher, H. (1998). Transport of in situ mobilized colloidal particles in packed soil columns. *Environmental Science and Technology*, *32*(22), 3562–3569. https://doi.org/10.1021/es980356z

Hale, K. (2018). Streamflow Sensitivity to Climate Warming and a Shift from Snowfall to Rainfall Streamflow sensitivity to climate warming and a shift from snowfall to.

Heindel, RC, Hinckley, ES, Murphy, SF, Repert, DA, and Anderson, SP (2018): Quantifying atmospheric dust deposition to the Colorado Front Range. Abstract A21I-0119 presented at 2018 *Fall Meeting, AGU*, Washington, DC, 10-14 Dec.

Hinckley, E. L. S., Ebel, B. A., Barnes, R. T., Anderson, R. S., Williams, M. W., & Anderson, S. P. (2012). Aspect control of water movement on hillslopes near the rain-snow transition of the Colorado Front Range. *Hydrological Processes*, *28*(1), 74–85. https://doi.org/10.1002/hyp.9549

Hinckley, E.-L. S., Barnes, R. T., Anderson, S. P., Williams, M. W., & Bernasconi, S. M. (2014). Nitrogen retention and transport differ by hillslope aspect at the rain-snow transition of the Colorado Front Range. *Journal of Geophysical Research: Biogeosciences*, 1281–1296. https://doi.org/10.1002/2013JG002588.Received

Hinckley, E. L. S., Ebel, B. A., Barnes, R. T., Murphy, S. F., & Anderson, S. P. (2017). Critical zone properties control the fate of nitrogen during experimental rainfall in montane forests of the Colorado Front Range. *Biogeochemistry*, *132*(1–2), 213–231. https://doi.org/10.1007/s10533-017-0299-8

Hongve, D. (1987). A revised procedure for discharge measurement by means of the salt dilution method. *Hydrological Processes*, *1*(3), 267–270.

Kampf, S. K., & Lefsky, M. A. (2016). Transition of dominant peak flow source from snowmelt to rainfall along the Colorado Front Range: Historical patterns, trends, and lessons from the 2013 Colorado Front Range floods. *Water Resources Research*, *52*(1), 407–422. https://doi.org/10.1002/2015WR017784

Kelly, P. J. (2012). Subsurface Evolution: Characterizing the physical and geochemical changes in weathered bedrock of Lower Gordon Gulch, Boulder Creek Critical Zone Observatory, 108.

Kim, H., Gu, X., & Brantley, S. L. (2018). Particle fluxes in groundwater change subsurface shale rock chemistry over geologic time. *Earth and Planetary Science Letters*, *500*, 180–191. https://doi.org/10.1016/j.epsl.2018.07.031

Koch, S., Kahle, P., & Lennartz, B. (2016). Visualization of Colloid Transport Pathways in Mineral Soils Using Titanium(IV) Oxide as a Tracer. *Journal of Environment Quality*, *45*(6), 2053. https://doi.org/10.2134/jeq2016.04.0131

Kretzschmar, R., & Sticher, H. (1997). Transport of humic-coated iron oxide colloids in a sandy soil: Influence of Ca2+ and trace metals. *Environmental Science and Technology*, *31*(12), 3497–3504. https://doi.org/10.1021/es970244s

Langston, A. L., Tucker, G. E., Anderson, R. S., & Anderson, S. P. (2015). Evidence for climatic and hillslope-aspect controls on vadose zone hydrology and implications for saprolite weathering. *Earth Surface Processes and Landforms*, *40*(9), 1254–1269. https://doi.org/10.1002/esp.3718

Lawrence, C. R., Reynolds, R. L., Ketterer, M. E., & Neff, J. C. (2013). Aeolian controls of soil geochemistry and weathering fluxes in high-elevation ecosystems of the Rocky Mountains, Colorado. *Geochimica et Cosmochimica Acta*, *107*, 27–46. https://doi.org/10.1016/j.gca.2012.12.023

Mills, T. J., Anderson, S. P., Bern, C., Aguirre, A., & Derry, L. A. (2017). Colloid Mobilization and Seasonal Variability in a Semiarid Headwater Stream. *Journal of Environment Quality*, *46*, 88–95. https://doi.org/10.2134/jeq2016.07.0268

Mills, T. J. (2016). Water Chemistry Under a Changing Hydrologic Regime : Investigations into the Interplay Between Hydrology and Water-Quality in Arid and Semi- Arid Watersheds in Colorado, USA.

Quénard, L., Samouëlian, A., Laroche, B., & Cornu, S. (2011). Lessivage as a major process of soil formation: A revisitation of existing data. *Geoderma*, *167–168*, 135–147. https://doi.org/10.1016/j.geoderma.2011.07.031

Séquaris, J. M., Klumpp, E., & Vereecken, H. (2013). Colloidal properties and potential release of water-dispersible colloids in an agricultural soil depth profile. *Geoderma*, *193–194*, 94–101. https://doi.org/10.1016/j.geoderma.2012.10.014

Trostle, K. D., Ray Runyon, J., Pohlmann, M. A., Redfield, S. E., Pelletier, J., McIntosh, J., & Chorover, J. (2016). Colloids and organic matter complexation control trace metal concentration-discharge relationships in

Marshall Gulch stream waters. *Water Resources Research*, *52*(10), 7931–7944. https://doi.org/10.1002/2016WR019072

USDA. (2016). Custom Soil Resource Report for Arapaho-Roosevelt National Forest Area, Colorado, Parts of Boulder, Clear Creek, Gilpin, Grand, Park and Larimer Counties, Gordon Gulch. *United States Department of Agriculture, Natural Resource Conservation Service*.

Veblen, T. T., Kitzberger, T., & Donnegan, J. (2000). Climatic and human influences on fire regimes in ponderosa pine forests in the colorado front range. *Ecological Applications*, *10*(4), 1178–1195. https://doi.org/10.1890/1051-0761(2000)010[1178:CAHIOF]2.0.CO;2

Wan, J., & Tokunaga, T. K. (1997). Film straining of colloids in unsaturated porous media: Conceptual model and experimental testing. *Environmental Science and Technology*, *31*(8), 2413–2420. https://doi.org/10.1021/es970017q

Zhang, Q., Knowles, J. F., Barnes, R. T., Cowie, R. M., Rock, N., & Williams, M. W. (2018). Surface and subsurface water contributions to streamflow from a mesoscale watershed in complex mountain terrain. *Hydrological Processes*, *32*(7), 954–967. https://doi.org/10.1002/hyp.11469

Zhang, W., Tang, X. Y., Weisbrod, N., Zhao, P., & Reid, B. J. (2015). A coupled field study of subsurface fracture flow and colloid transport. *Journal of Hydrology*, *524*, 476–488. https://doi.org/10.1016/j.jhydrol.2015.03.001

Zhang, W., Tang, X. Y., Xian, Q. S., Weisbrod, N., Yang, J. E., & Wang, H. L. (2016). A field study of colloid transport in surface and subsurface flows. *Journal of Hydrology*, *542*, 101–114. https://doi.org/10.1016/j.jhydrol.2016.08.056

Appendix A: Soil water data

Soil water was collected during spring and early summer of 2018. I used zero tension lysimeters installed and described by Hinckley et al. (2012; 2014; 2017). Bottles were replaced every 1-2 weeks. Water was filtered through a 0.45 micron filter, stored at 4° C, and analyzed as described in the methods section.

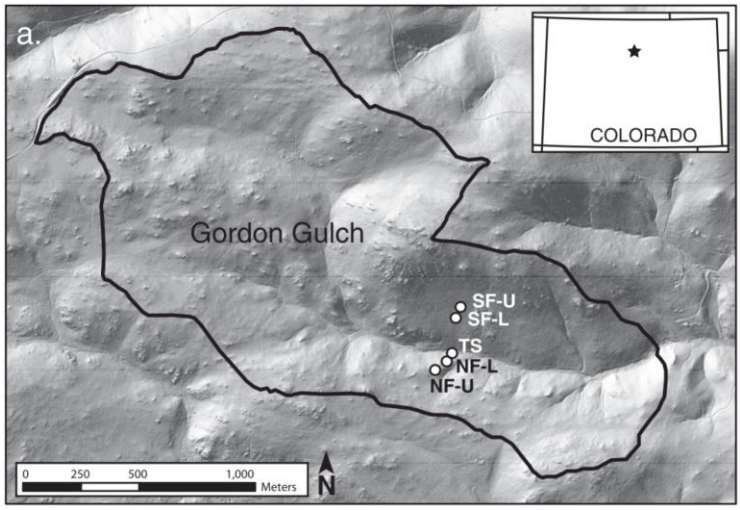

Figure A1. Location of zero tension lysimeters (from Hinckley et al., 2012)

Table A1. Soil water data, spring and summer 2018.

Location	Lysimeter Site Name	Depth	Date in field	Date out of field	Date filtered	Si (ppm)	Mg^{2+} (ppm)	Ca^{2+} (ppm)	Al (ppm)	Na^{+} (ppm)	K^{+} (ppm)	pH	Alk (meq/L)	Alk (mg/L)	Cl^{-} (ppm)	SO_4^{2-} (ppm)
SF-U	M1	30	4/26/18	5/11/18	5/15/18	1.93	2.30	12.33	0.52	1.50	3.95	7.22	0.57	28.50	0.44	2.31
SF-L	M2	10	4/26/18	5/11/18	5/15/18	1.94	1.21	3.19	1.27	1.07	8.05	6.34	0.17	8.70	1.37	1.25
SF-L	M2	27	4/26/18	5/11/18	5/15/18	4.46	1.78	4.46	1.60	1.29	2.88	6.91	0.27	13.40	0.09	0.45
TS	M3	21	4/26/18	5/8/18	5/15/18	4.32	1.15	3.54	1.43	2.40	5.25	6.33	0.18	8.60	2.64	0.88
TS	M3	25	4/26/18	5/8/18	5/15/18	5.13	1.76	7.62	2.38	1.11	5.13	5.96	0.17	9.00	1.94	1.58
NF-U	M5	42	4/26/18	5/11/18	5/17/18	8.70	1.71	4.72	2.20	1.23	0.95	5.49	0.09	4.60	0.31	1.39
SF-U	R1	23.5	4/26/18	5/11/18	5/15/18	1.72	1.16	4.24	1.37	0.47	4.20	6.64	0.23	11.30	0.35	0.16
SF-L	R2	16	4/26/18	5/11/18	5/15/18	2.07	2.07	7.65	0.07	0.53	3.05	7.03	0.40	20.10	1.00	2.40
SF-L	R2	17	4/26/18	5/11/18	5/17/18	1.88	1.29	3.53	0.15	1.79	17.26	7.20	0.51	25.60	0.44	1.29
NF-L	R4	24	4/26/18	5/11/18	5/15/18	3.61	0.87	3.59	1.72	1.65	1.02	6.62	0.18	9.15	0.49	0.62
NF-L	R4	25	4/26/18	5/11/18	5/17/18	1.55	0.80	4.24	1.53	0.47	1.37	6.45	0.15	7.50	0.19	0.74
NF-U	R5	17	4/26/18	5/11/18	5/15/18	4.11	1.13	3.38	1.17	1.17	1.17	5.94	0.08	10.50	0.21	0.78
NF-U	R5	40	4/26/18	5/11/18		5.08	1.06	3.45	1.83	1.21	2.02	5.89	0.08	3.90	3.24	1.44
SF-U	M1	14	5/11/18	5/16/18	5/17/18	1.47	1.13	4.33	0.22	0.46	2.76	7.01	0.18	10.50	0.45	0.39
SF-U	R1	23.5	5/11/18	5/16/18	5/17/18	2.12	1.46	6.20	0.82	0.57	5.99	6.49	0.28	13.90	0.34	0.21
SF-L	R2	16	5/11/18	5/16/18	5/17/18	1.79	1.77	7.05	0.11	1.04	3.74	7.25	0.48	24.20	0.59	0.24
NF-L	R4	24	5/11/18	5/16/18	5/17/18	3.56	0.89	3.91	1.81	2.28	2.70				2.08	0.95

SF-U	M1	14	5/16/18	5/31/18	6/9/18	1.65	1.15	4.52	0.29	0.39	3.09	6.83	0.21	10.40	0.39	0.15
SF-U	M1	30	5/16/18	5/31/18	6/9/18	1.77	2.33	12.44	0.18	1.09	3.22	7.46	0.61	30.30	0.86	1.79
NF-U	M5	42	5/16/18	5/31/18	6/9/18	6.65	2.10	6.06	1.36	2.82	2.70				0.00	0.00
SF-U	R1	23.5	5/16/18	5/31/18	6/9/18	1.44	1.47	6.21	1.55	0.55	6.01	6.59	0.27	13.60	0.25	0.12
SF-L	R2	16	5/16/18	5/31/18	6/9/18	1.87	1.72	6.63	0.08	0.52	3.23	7.21	0.46	22.80	0.15	0.24
SF-L	R2	17	5/16/18	5/31/18	6/9/18	0.34	0.22	0.78	0.02	0.75	2.65				0.00	0.00
TS	R3	12.5	5/16/18	5/31/18	6/9/18	4.45	1.07	4.39	0.79	0.76	2.49				1.34	0.19
NF-L	R4	24	5/16/18	5/31/18	6/9/18	1.67	0.85	3.14	0.52	2.44	5.69				0.00	0.00
NF-U	R5	17	5/16/18	5/31/18	6/9/18	1.32	0.54	1.68	0.44	0.51	1.10	5.72			0.62	0.52
NF-U	R5	40	5/16/18	5/31/18	6/9/18	3.38	0.94	2.98	0.76	1.72	3.04				0.00	0.00
TS	R3	20	6/4/18	6/14/18	6/15/18	4.71	0.86	3.40	0.35	0.59	1.30	6.31	0.10	4.60	0.25	1.02
NF-L	R4	25	6/4/18	6/14/18	6/15/18	8.13	1.64	6.48	2.82	1.16	3.29				3.18	1.28
NF-L	R4	35	6/4/18	6/14/18	6/15/18	6.08	1.72	6.49	2.15	1.35	2.21				0.76	1.08
SF-U	M1	14	6/14/18	6/19/18	6/21/18	1.55	1.78	6.77	0.30	0.34	3.81	6.38	0.25	12.70	2.43	0.69
SF-U	R1	23.5	6/14/18	6/19/18	6/21/18	3.99	2.20	8.43	2.12	0.77	8.40	6.30	0.31	15.60	3.28	1.14
SF-L	R2	16	6/14/18	6/19/18	6/21/18	1.99	1.67	4.18	0.09	2.28	8.82				1.08	1.31
SF-L	R2	17	6/14/18	6/19/18	6/21/18	1.66	3.32	12.75	0.09	0.58	4.80	6.89	0.40	20.10	6.17	5.64
TS	R3	20	6/14/18	6/19/18	6/21/18	3.37	0.94	3.68	0.32	1.59	1.18				0.00	0.00
TS	R3	27	6/14/18	6/19/18	6/21/18	4.65	1.12	3.15	2.80	1.07	4.20	6.43	0.19	9.40	0.95	0.55
NF-L	R4	25	6/14/18	6/19/18	6/21/18	7.33	1.25	4.81	1.69	1.18	2.76				0.00	0.00
NF-U	R5	17	6/14/18	6/19/18	6/21/18	1.35	1.08	3.45	0.92	0.84	2.21	5.92	0.07	4.90	0.86	0.56

Appendix B: Centrifuged surface and groundwater data

I analyzed surface and groundwater samples from spring and summer 2018 for colloidal material. In spring and summer 2018 BcCZO staff collected extra surface and groundwater samples at the same time as standard BcCZO monitoring samples so that the samples can be compared (see methods section). I processed these samples in accordance with BcCZO standard protocols and added a centrifugation step to remove colloids. This step was added after filtering through 0.45 micron filters and before sample analysis in the BcCZO and LEGS laboratories. I centrifuged samples for 6 hours at 2000 rpm. This is a departure from Mills et al. (2017) and Aguirre et al. (2017), who centrifuged for 4.5 hours at 8000 rpm. The following data comprises centrifuged samples, which can be compared to publicly available BcCZO sample data to calculate colloid and dissolved concentrations.

Table B1. Centrifuged surface and groundwater data, spring and summer 2018.

Site	Date Collected	Date Filtered	Si (ppm)	Mg (ppm)	Ca (ppm)	Al (ppm)	Na (ppm)	K (ppm)
GGL_SW_0	5/7/18	5/14/18	6.464	2.209	5.844	0.357	2.858	0.996
GGU_SPW_1	5/11/18	5/14/18	6.025	2.027	3.431	1.248	2.228	1.054
GGU_SW_0	5/11/18	5/14/18	6.477	1.821	4.285	0.482	2.526	0.895
GGU_SPW_2	5/11/18	5/14/18	6.480	2.220	5.037	0.293	2.482	1.303
GGL_SW_0	5/15/18	5/17/18	7.187	2.404	6.309	0.564	2.989	1.003
GGU_SW_2	5/15/18	5/17/18	6.659	2.339	5.199	0.141	2.581	1.364
GGU_SW_0	5/15/18	5/17/18	6.717	1.901	4.577	0.474	2.570	0.878
GGU_SW_0	5/24/18	6/9/18	6.616	1.916	4.581	0.277	2.632	0.859
GGL_SW_0	5/29/18	6/9/18	6.974	2.483	6.467	0.462	3.049	1.071
GGL_SW_0	6/1/18	6/9/18	6.316	2.021	4.863	0.234	2.628	0.798
GGL_IS_WF_11	6/1/18	6/9/18	6.516	2.340	6.094	0.235	2.866	0.954
GGU_SPW_1	6/1/18	6/9/18	5.336	2.310	4.050	0.047	2.328	1.025
GGU_SW_0	6/1/18	6/9/18	6.656	2.615	6.762	0.221	3.105	0.967
GGU_SPW_3	6/1/18	6/9/18	6.458	2.236	4.988	0.284	2.461	1.265
GGU_IS_WF_9	6/1/18	6/9/18	5.705	2.168	5.236	0.178	2.550	1.117
GGU_SPW_1	6/7/18	6/9/18	5.751	1.750	4.802	0.166	2.554	1.151
GGL_SW_0	6/7/18	6/9/18	6.987	2.762	7.562	0.155	3.382	1.097
GGU_SW_0	6/7/18	6/9/18	6.594	2.195	5.262	0.273	2.769	0.774
GGU_SPW_2	6/7/18	6/9/18	6.948	2.339	5.166	0.341	2.511	1.351
GGL_IS_WF_11	6/14/18	6/15/18	6.744	2.550	6.656	0.160	3.178	1.202
GGU_IS_WF_9	6/7/18	6/15/18	5.553	2.189	5.432	0.119	2.533	1.119

GGU_IS_SF_1	6/14/18	6/15/18	5.822	3.065	7.564	0.150	3.237	1.781
GGL_SW_0	6/14/18	6/15/18	6.883	2.990	8.076	0.065	3.517	1.091
GGU_SPW_2	6/14/18	6/15/18	6.634	2.344	5.097	0.217	2.497	1.281
GGU_SW_0	6/14/18	6/15/18	6.402	2.413	5.684	0.179	2.807	1.393
GGU_SPW_1	6/14/18	6/15/18	4.708	0.862	3.396	0.349	0.589	1.301
GGU_IS_NF_9	6/14/18	6/15/18	1.547	1.778	6.769	0.298	0.340	3.812